PHYSICAL REVIEW B VOLUME 32, NUMBER 10 15 NOVEMBER 1985

Theory of exciton-phonon coupling in one-dimensional molecular crystals: A variational treatment with delocalized solitary states

Gerd Venzl* and Sighart F. Fischer
Technische Universität München, Physik Department, 8046 Garching, Germany
(Received 3 August 1984; revised manuscript received 3 June 1985)

A one-dimensional model of Frenkel excitons and dispersionless phonons interacting via a linear site-diagonal coupling term is investigated. We present a variational theory which is, for explicit calculations, reduced to two variational parameters characterizing the excitonic coherence properties as well as the extent of lattice distortion. It includes previous theories (phonon-dressed excitons and adiabatic solitary solutions) as limiting cases. The theory fully accounts for the translation symmetry and is applicable in the weak-coupling and the self-trapping regions of the physical parameter space as well as in the crossover regime. Energetic and spectroscopic properties of the full (k-dependent) phonon-free exciton band are calculated. Important results are the band deformation due to the interaction with multiphonon states of the same symmetry, the exciton dispersion, and strong variations of the intensities and the degree of localization within the exciton band.

I. INTRODUCTION

The problem of exciton-phonon interactions and their effect on the spectra and transport properties of molecular crystals has caught the interest of physicists and physical chemists for many years.[1–3] Generally, electronic excitations of molecules in pure crystals tend to delocalize and form exciton bands due to the intermolecular resonance transfer. The interaction with phonons which modulate the electronic energy levels of the molecules has an opposing effect. An electronic excitation on a particular molecule can lower its energy by a rearrangement of the intramolecular and intermolecular nuclear coordinates. This destroys the resonance with neighboring sites and tends to stabilize the localized excitation. The competition between these two trends towards delocalization and localization leads to a substantially different behavior of the exciton depending on which of the two trends dominates. This is well manifested by the transition probabilities from the ground state into these excited states. The delocalized states get large Franck-Condon factors while the relaxed states have only small zero-phonon transition probabilities. In molecular crystals with two molecules per unit cell the upper band edge may get intensity. Therefore, it is of interest to study the dispersion of the exciton band.

To construct a simplified model let us consider an exciton in a one-dimensional crystal which is coupled to a dispersionless intramolecular vibration via a coupling term linear in the phonon coordinates. A corresponding Hamiltonian reads

$$H=\sum_n b_n^\dagger b_n+\lambda\sum_n(b_n^\dagger+b_n)a_n^\dagger a_n-V\sum_n a_n^\dagger(a_{n+1}+a_{n-1})\ . \tag{1}$$

The operators a_n and b_n are creation operators of excitons and phonons at site n, respectively. We have chosen the energy scale such that the frequency of the phonons is unity. There are two characteristic energies in the problem, i.e., the energy of localization or Stoke's shift λ^2 and the energy of delocalization $2V$. Their ratio measures the relative importance of the trends towards localization and delocalization. We shall restrict ourselves to the discussion of phenomena at low density of excitons and at zero absolute temperature.

Our approach to analyze certain properties of the interacting system defined by the Hamiltonian (1) is variational. This has a long tradition for the polaron as well as the exciton-phonon problems.[4–14] Variational trial wave functions discussed in the literature[5,7] include a superposition of exciton states dressed by phonon clouds consisting of displaced harmonic oscillators. In general, there are many variational parameters, those describing the superposition and those describing the lattice distortion. If only the latter is considered one can relate the wave-number-dependent lattice distortion to a single parameter which has to be determined in a self-consistent way. Such simplified models predict discontinuities in the transition probabilities as a function of λ^2 if the excitonic interaction V exceeds a critical parameter V_c. This is so even in the one-dimensional case, where such discontinuities should not occur as has been shown by studying the adiabatic ground state in the continuum limit.[7,9,11] For two and three dimensions discontinuities are predicted depending on the range of interaction.

As one introduces proper superpositions [see Refs. 5 and 7 and Eqs. (17) and (18) of this paper] the discontinuities in one dimension are removed for the parameter regime of λ^2 and V, where the simple dressed exciton theory shows discontinuities.

We show this explicitly by introducing two trial parameters. One of them is related to the width of solitary solutions, the other stands for the lattice distortion only. The choice of the trial functions is motivated by an approach to exciton-phonon systems which yields strictly localized (solitary) states states that break the translation symmetry of the Hamiltonian.[15–18] It turns out that these states yield a lower energy in the self-trapping regime than the simplified dressed exciton *ansatz* discussed above.[15] Obviously the solitary solutions represent more flexible local wave functions than those contained in the simple dressed exciton *ansatz*. Our idea is to use these local states but restore translation invariance by a coherent superposition of

the degenerate states. The optimization of the variational parameters is performed afterwards for each crystal wave number k separately. As a result we obtain the dispersion $E(k)$ of the exciton band as well as the intensities of the lowest exciton states as a function of wave number k and in the presence of exciton-phonon coupling. We are not aware of any theory which yields an equal amount of information on the energetic and spectroscopic properties of the exciton band. We further stress the fact that our theory contains the simple dressed exciton theory as well as the solitary solutions as limiting cases. Therefore it represents an improvement with respect to both of them and for the whole range of coupling parameters.

The organization of this paper is as follows. Section II introduces our variational trial function and its relation to those used previously. Section III discusses exact properties of this *ansatz*, whereas Sec. IV introduces additional restrictions on the variational parameters which reduce the problem to the optimization of the energy with respect to two parameters only. Section V presents selected numerical results on the crossover between mobile and self-trapped states as well as on the properties of the exciton band as a function of the resonance transfer and interaction parameters. Conclusions are given in Sec. VI.

II. VARIATIONAL TRIAL FUNCTIONS

In this section we briefly discuss two distinct variational approaches to exciton-phonon systems used previously. An obvious generalization which contains these theories as special cases leads to the variational trial function this work is based on.

The first approach uses the concept of a *"dressed exciton."* Due to exciton phonon coupling an electronic excitation carries with it a cloud of phonons or lattice distortions.[4-14] The most simple *ansatz* corresponding to this picture and specialized to the Hamiltonian (1) is

$$|k\rangle = N^{-1/2}\sum_n e^{-ikn}|n;\{\lambda_n(k)\}\rangle \tag{2}$$

with

$$|n;\{\lambda_n(k)\}\rangle = \exp\left[\sum_{n'}\lambda_{n'-n}(k)(b_{n'}^\dagger - b_{n'})\right]a_n^\dagger|0\rangle\ . \tag{3}$$

Here and in what follows $|0\rangle$ denotes the vacuum state for the excitons as well as the phonons. Note that this *ansatz* only specifies the form of the ground states with respect to the phonons but does not imply how vibrationally excited states should be constructed (compare Refs. 7 and 14 for different prescriptions).

The wave functions (2) are eigenstates of the total crystal wave-number operator

$$\hat{k} = \sum_{k'} k' a_{k'}^\dagger a_{k'} + \sum_q q b_q^\dagger b_q\ . \tag{4}$$

Since the Hamiltonian (1) is translation invariant there is no coupling between states of different k. Therefore the variational parameters $\lambda_{n'-n}(k)$ which describe the lattice distortion at site n' around an electronic excitation at site n can be optimized for each k separately. A systematic decomposition of the Hamiltonian (1) into a sum of pure phonon Hamiltonians acting on the invariant subspaces of total wave number can be performed using an appropriate unitary transformation. Together with the solution of the variational problem in terms of displaced oscillators this has been described in some recent publications for dispersionless phonons,[13,14] which is the case we exclusively treat in this paper, and for acoustical phonons.[15] We cite the main results in a form appropriate for further reference in this paper. The optimized distortion parameters are

$$\lambda_n(k) = -\lambda\frac{1-\delta(k)}{1+\delta(k)}[\delta(k)]^n\ , \tag{5}$$

where $\delta(k)$ is related to a generalized Debye-Waller factor $R(k)$ via

$$\delta(k) = \frac{\sqrt{1+4VR(k)\cos k}-1}{\sqrt{1+4VR(k)\cos k}+1} \tag{6}$$

which in turn fulfills the self-consistency relation

$$R(k) = \exp\{-\lambda^2[1+4VR(k)\cos k]^{-3/2}\}\ . \tag{7}$$

Thus, the problem can be reduced to the solution of a single transcendental equation for $R(k)$.

A different theory for the ground state of the exciton-phonon Hamiltonian (1) may be based on Davydov's *ansatz*[17]

$$|n;\{\varphi_n\},\{\lambda_n\}\rangle = \sum_{n'}\varphi_{n'-n}\exp\left[\sum_{n''}\lambda_{n''-n}(b_{n''}^\dagger - b_{n''})\right]a_{n'}^\dagger|0\rangle \tag{8}$$

with variational parameters φ_n and λ_n representing excitonic amplitudes and lattice distortions, respectively. Normalization of the wave function implies

$$\sum_n |\varphi_n|^2 = 1\ . \tag{9}$$

The expectation value of the Hamiltonian for the states (8) yields the energy functional

$$\mathcal{H}(\{\varphi_n\},\{\lambda_n\}) = \sum_n \lambda_n^2 + 2\lambda\sum_n \lambda_n|\varphi_n|^2 - V\sum_n \varphi_n^*(\varphi_{n+1}+\varphi_{n-1})\ . \tag{10}$$

It is extremal with respect to the λ_n if

$$\lambda_n = -\lambda|\varphi_n|^2 \tag{11}$$

is fulfilled. This relation allows the elimination of the lattice distortion parameters λ_n to yield an energy functional expressed in terms of the φ_n alone,

$$\mathcal{H}'(\{\varphi_n\}) = -\lambda^2\sum_n |\varphi_n|^4 - V\sum_n \varphi_n^*(\varphi_{n+1}+\varphi_{n-1})\ . \tag{12}$$

For long chains the ground state based on the *ansatz* (8) is a localized or *"solitary" solution* centered at arbitrary sites n. The amplitudes $\varphi_{n'-n}$ obey the symmetry relation

$$\varphi_{n'-n} = \varphi_{n-n'} \tag{13}$$

and decay exponentially for $|n'-n| \to \infty$. In the continuum limit, which is equivalent to the relation $\lambda^2 \ll 2V$, one has the well-known solution[16,19]

$$\varphi_{n'-n} \approx \left[\frac{\lambda^2}{4V}\right]^{1/2} \operatorname{sech}\left[\frac{\lambda^2}{2V}(n'-n)\right] . \tag{14}$$

In the strong-coupling limit ($\lambda^2 \gg 2V$) the excitonic amplitudes have the form of a geometric series

$$\varphi_{n'-n} \approx \frac{1-\epsilon^2}{1+\epsilon^2}\epsilon^{|n'-n|} . \tag{15}$$

Minimization of the energy functional $\mathscr{H}'$, Eq. (12), with respect to ϵ yields in lowest order

$$\epsilon = \frac{V}{2\lambda^2} + O\left[\frac{V^2}{\lambda^4}\right] . \tag{16}$$

A solution for intermediate-coupling strengths ($\lambda^2 \gtrsim 2V$) can be obtained by means of an iterative solution applied recently to the problem of an excitation coupled to acoustical phonons.[15]

The prominant difference between the two distinct trial functions (2), (3), and (8) is the following: The "dressed exciton" solution (2) is a coherent superposition of certain local wave functions given by (3). Therefore it is an eigenstate of the total crystal momentum operator which commutes with the total Hamiltonian. The weakness of this approach is due to the simple structure of the local wave function (3). On the other hand, the *ansatz* (8) which leads to solitary states breaks the symmetry which corresponds to momentum conservation and leads to a highly degenerate ground state. Our notation in (8) intends to make clear that these states present a particular way to model more sophisticated local wave functions. If $\varphi_{n-n'} = \delta_{n'n}$, i.e., $\varphi_{n'-n}$ vanishes unless $n'=n$, Eq. (8) is identical to the simpler local wave function (3). Coherent superposition restores translation invariance of the wave function and leads to our generalized trial function

$$|k\rangle = N^{-1/2} \sum_n e^{-ikn} |n;\{\varphi_n(k)\},\{\lambda_n(k)\}\rangle \tag{17}$$

with

$$|n;\{\varphi_n(k)\},\{\lambda_n(k)\}\rangle = \sum_{n'} \varphi_{n'-n}(k) \exp\left[\sum_{n''} \lambda_{n''-n}(k)(b_{n''}^\dagger - b_{n''})\right] a_{n'}^\dagger |0\rangle . \tag{18}$$

This defines the variational problem, which has been formulated also by Toyozawa[5] for a slightly different model Hamiltonian. However, Toyozawa immediately introduces the approximation $\varphi_{n-n'} = \delta_{n-n'}$ which corresponds to the *ansatz* equations (2) and (3). We shall consider for explicit calculations a more general form for the excitonic amplitudes, namely the *ansatz* (32) presented in Sec. IV.

In order to elucidate the relation to the dressed exciton picture we rewrite the trial function [Eqs. (17) and (18)] in the following way:

$$|k\rangle = N^{-1/2} \sum_n e^{-ikn} \Phi_n^{(k)}(\{b_n^\dagger, b_n\}) a_n^\dagger |0\rangle . \tag{19}$$

This is the most general form of any one-exciton solution to the Hamiltonian (1). The operator $\Phi_n^{(k)}(\{b_n^\dagger, b_n\})$ contains the dressing of the exciton as well as possible vibrational excitations of the crystal. The trial function corresponds to the special choice

$$\Phi_n^{(k)}(\{b_n^\dagger, b_n\}) = \sum_{n'} e^{ikn'} \varphi_{n'} \exp\left[\sum_{n''} \lambda_{n''+n'-n}(b_{n''}^\dagger - b_{n''})\right] . \tag{20}$$

The flexibility of the wave function in comparison with the simple dressed exciton *ansatz*, Eq. (2) and (3), stems from the fact that a sum of displaced oscillator functions is considered instead of only one term. This includes the possibility to account for the increased (static) fluctuations $\langle (x_n - \langle x_n \rangle)^2 \rangle$ of the oscillator coordinates $x_n \propto b_n^\dagger + b_n$ in the crossover regime.[8]

III. EXACT RELATIONS

The reader who is mainly interested in the method and the results may skip over this section in which some exact results for the trial function [Eqs. (17) and (18)] and the corresponding variational problem are derived. We prove an exact sum rule for the lattice distortion parameters $\lambda_n(k)$ and the existence of a particular upper bound for the energy $E(k)$. For simplicity of notation we cease from indicating the k dependence of the variational parameters.

For future use we first calculate the following matrix elements:

$$\langle k|k'\rangle = \delta_{kk'} \sum_n e^{ikn} F_n \sum_{n'} \varphi_{n'}^* \varphi_{n'+n} , \tag{21}$$

$$\langle k|H_{\rm ph}|k'\rangle = \delta_{kk'} \sum_n e^{ikn} F_n \sum_{n'} \varphi_{n'}^* \varphi_{n'+n} \sum_{n''} \lambda_{n''} \lambda_{n''+n} , \tag{22a}$$

$$\langle k|H_{\rm int}|k'\rangle = \lambda \delta_{kk'} \sum_n e^{ikn} F_n \sum_{n'} \varphi_{n'}^* \varphi_{n'+n} (\lambda_{n'} + \lambda_{n'+n}) , \tag{22b}$$

$$\langle k|H_{\rm ex}|k'\rangle = -V\delta_{kk'} \sum_n e^{ikn} F_n \sum_{n'} \varphi_{n'}^* (\varphi_{n'+n-1} + \varphi_{n'+n+1}) . \tag{22c}$$

Evidently $H_{\rm ph}$, $H_{\rm int}$, and $H_{\rm ex}$ denote the individual contributions to the total Hamiltonian (1). The F_n are the Franck-Condon factors between the phonon part of the local wave function (18) and a corresponding state shifted by n lattice sites. They are given by

$$F_n = \exp\left[\sum_{n'} (\lambda_{n'} \lambda_{n'+n} - \lambda_{n'}^2)\right] . \tag{23}$$

Obviously F_n is an even function of n, i.e., $F_{-n} = F_n$, and $F_0 = 1$. Equations (21) and (22) verify that the trial functions for different k are orthogonal and not coupled by the Hamiltonian. The relation to the two limiting cases discussed in the preceding section is the following. As has

been noted, the simple dressed exciton picture is obtained for $\varphi_n=\delta_{n0}$. In this case only F_1 enters which is equal to the band reduction factor R, Eq. (7). If vibrational overlap between shifted lattice states is neglected, i.e., $F_n=\delta_{n0}$, the expectation value of the Hamiltonian is identical to the energy functional (10) which leads to the solitary ground-state solutions.

Next we derive the sum rule

$$\sum_n \lambda_n = -\lambda \ , \tag{24}$$

which holds for the optimized lattice distortions λ_n. It may be guessed because it is fulfilled for the corresponding quantities in the theories discussed in Sec. II, compare eq. (5) and (11). In order to derive (24) we perform the variation of

$$\mathscr{H}(\{\varphi_n\},\{\lambda_n\},\eta)=\langle k\mid H\mid k\rangle+\eta(\langle k\mid k\rangle-1) \tag{25}$$

with respect to say λ_m. A Lagrange parameter η has been included to assure normalization. The result is

$$0=\frac{\partial\mathscr{H}}{\partial\lambda_m}=\sum_n e^{ikn}F_n\left[(\lambda_{m+n}+\lambda_{m-n})\sum_{n'}\varphi^*_{n'}\varphi_{n'+n}+\lambda(\varphi^*_m\varphi_{m+n}+\varphi^*_{m-n}\varphi_m)\right]+\sum_n e^{ikn}\frac{\partial F_n}{\partial\lambda_m}[\cdots] \ . \tag{26}$$

The last term in this equation is just $\mathscr{H}$ as given by (25) and Eqs. (19) and (20a)—(20c) if only F_n is replaced by $\partial F_n/\partial\lambda_m$ throughout. Now we sum over all m and note that

$$\sum_m \frac{\partial F_n}{\partial\lambda_m}=\sum_m(\lambda_{m+n}+\lambda_{m-n}-2\lambda_m)F_n=0 \ . \tag{27}$$

The result is

$$0=2\left[\sum_m\lambda_m+\lambda\right]\sum_n e^{ikn}F_n\sum_{n'}\varphi^*_{n'}\varphi_{n'+n}=2\left[\sum_m\lambda_m+\lambda\right] . \tag{28}$$

The last equation follows from normalization, compare (21). This completes the derivation of the sum rule (24). It will be useful in the following section in order to reduce the number of independent variational parameters.

Finally we show that the energies corresponding to the optimized wave functions fulfill the inequality

$$E(k)\le\begin{cases}-2V & \text{for } k=0,\\ -2V+1 & \text{for } k\neq 0.\end{cases} \tag{29}$$

This inequality is most easily understood in the limit of weak coupling ($\lambda^2\ll 1$) and if the bare exciton bandwidth $4V$ is greater than the phonon frequency which is unity in our units of energy ($4V>1$). For $k=0$ the upper bound is just the bare excition band bottom. For $k\neq 0$ the lowest state with a given total wave number k is approximately given by an exciton of wave number $k_{\rm ex}=0$ with energy $\epsilon_{\rm ex}\ (k_{\rm ex}=0)=-2V$ plus an optical phonon with wave number $k_{\rm ph}=k$ and energy $\epsilon_{\rm ph}\ (k_{\rm ph})=1$. Then the total wave number is $k=k_{\rm ex}+k_{\rm ph}$ and the total energy $E(k)=\epsilon_{\rm ex}(0)+\epsilon_{\rm ph}(k)=-2V+1$. The inequality (29) is, of course, trivial for exact solutions. We find it remarkable, however, that it is fulfilled for our variational trial functions. For the simple dressed exciton solutions discussed in Sec. II the lower part of (29) is not fulfilled if $4V>1$ holds.

In order to prove (29), we show that for a particular choice of our variational parameters φ_n and λ_n, the right-hand side is obtained as the expectation value of the Hamiltonian. Guided by the explanation given above we choose $\varphi_n=N^{-1/2}$ which constructs a bare exciton of wave number $k=0$. (N is the total number of lattice sites.) Using Eqs. (21)—(23), we find

$$\langle H\rangle_k\equiv\frac{\langle k\mid H\mid k\rangle}{\langle k\mid k\rangle}=-2V-\frac{2\lambda^2}{N}+\frac{\sum_{n,n'}e^{ikn}\lambda_{n'}\lambda_{n'+n}\exp\left[\sum_{n''}\lambda_{n''}\lambda_{n''+n}\right]}{\sum_n e^{ikn}\exp\left[\sum_{n''}\lambda_{n''}\lambda_{n''+n}\right]} \ . \tag{30}$$

If we further assume that the λ_n are sufficiently small such that the exponential may be expanded to first order, we obtain

$$\langle H\rangle_k\approx -2V\frac{2\lambda^2}{N}+\frac{\sum_{n,n'}e^{ikn}\lambda_{n'}\lambda_{n'+n}}{N\delta_{k0}+\sum_{n,n'}e^{ikn}\lambda_{n'}\lambda_{n'+n}} \ . \tag{31}$$

This implies the upper bound (29) in the limit of large N.

IV. APPROXIMATE SOLUTION OF THE VARIATIONAL PROBLEM

Our trial function [Eqs. (17) and (18)] contains $2N$ variational parameters. This number can be reduced to $2N-2$ independent parameters by means of normalization and the sum rule (24). There is no principal difficulty to solve the variational problem numerically for large but finite N. Nevertheless we found it more instructive and sufficient for many purposes to introduce additional approximations which reduce the number of independent parameters to two only. Guided by the behavior of the solutions in the dressed exciton and soliton limits discussed in Sec. II we choose an *ansatz* as geometric series for φ_n and λ_n,

$$\varphi_n=C\left[\frac{1-\epsilon^2}{1+\epsilon^2}\right]^{1/2}\epsilon^{|n|} \ , \tag{32}$$

$$\lambda_n=-\lambda\frac{1-\delta}{1+\delta}\delta^{|n|} \ . \tag{33}$$

Equation (33) is identical in form with (5) so that the

dressed exciton problem is recovered for $\epsilon=0$. On the other hand, the geometric series *ansatz* for φ_n represents a fairly good approximation to the solitary solution in the case of intermediate and strong coupling ($\lambda^2 \gtrsim 4V$).[20] Moreover, Eqs. (32) and (33) are consistent for the soliton because $\lambda_n \propto |\varphi_n|^2$ holds in this case, compare (11). The fact that (32) is not a good approximation to the continuum solution (14) which holds for weak coupling does not appear to be a severe drawback. In this limit one can show that the dressed exciton solution is superior to the soliton at least if the lower ground-state energy is taken as the criterion.[20] Summarizing, we expect the parametrization [Eqs. (32) and (33)] to contain and improve both types of theories. It fulfills the sum rule (24) and reduces the problem to the optimization of the expectation value $\langle H \rangle_k$ of the Hamiltonian with respect to the two parameters ϵ and δ. The energy function $\langle H \rangle_k$ does not depend on the normalization constant C in (32).

By means of Eqs. (32) and (33) we can analytically evaluate the matrix elements [Eqs. (21) and (22a)—(22c)], except for one summation which has to be done numerically,

$$\langle k \mid k \rangle = C^2 \left[1+2 \sum_{n=1}^{\infty} \cos(kn) F_n f_n(\epsilon) \right] , \tag{34}$$

$$\langle k \mid H_{\rm ph} \mid k \rangle = C^2 \lambda^2 \frac{(1-\delta)(1+\delta^2)}{(1+\delta)^3} \left[1+2 \sum_{n=1}^{\infty} \cos(kn) F_n f_n(\epsilon) f_n(\delta) \right] , \tag{35a}$$

$$\langle k \mid H_{\rm int} \mid k \rangle = -2C^2 \lambda^2 \frac{1-\epsilon^2}{(1+\epsilon^2)(1+\delta)(1-\epsilon^2\delta)} \left[(1-\delta)(1+\epsilon^2\delta)+2 \sum_{n=1}^{\infty} \cos(kn) F_n g_n(\epsilon,\delta) \right] , \tag{35b}$$

$$\langle k \mid H_{\rm ex} \mid k \rangle = -2C^2 V \left[\frac{2\epsilon}{1+\epsilon^2} + \sum_{n=1}^{\infty} \cos(kn) F_n [f_{n-1}(\epsilon)+f_{n+1}(\epsilon)] \right] . \tag{35c}$$

The auxiliary functions f_n and g_n are defined as

$$f_n(x) = x^n \left[1 - \frac{1-x^2}{1+x^2} n \right] , \tag{36}$$

$$g_n(x,y) = x^n [1-x^2y^2-(1-x^2)y^{1+n}] . \tag{37}$$

Using f_n we find

$$F_n = \exp \left[-\lambda^2 \frac{(1-\delta)(1+\delta^2)}{(1+\delta)^3} [1-f_n(\delta)] \right] \tag{38}$$

for the local Franck-Condon factors.

Since the energy function to be minimized depends on two variational parameters only its behavior can easily be displayed graphically by means of contour plots. Figures 1—3 show the energy for the ground state $k=0$ and three selected examples, namely a constant intermolecular transfer $V=2$ and different exciton-phonon coupling strengths $\lambda^2=1$ (Fig. 1), $\lambda^2=6.25$ (Fig. 2), and $\lambda^2=10$

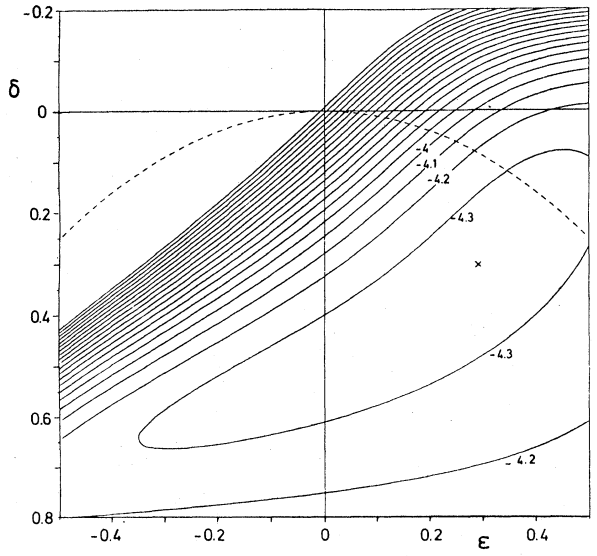

FIG. 1. Energy expectation value for the trial function [Eqs. (17) and (18)] with $k=0$ and the simplifying geometric series *ansatz* [Eqs. (32) and (33)] as a function of the variational parameters ϵ and δ. Curves of constant energy (solid lines), the energy minimum (marked by a cross), and the soliton characteristic $\delta=\epsilon^2$ (dashed line) are depicted. The magnitudes of the physical parameters are $\lambda^2=1$ and $V=2$.

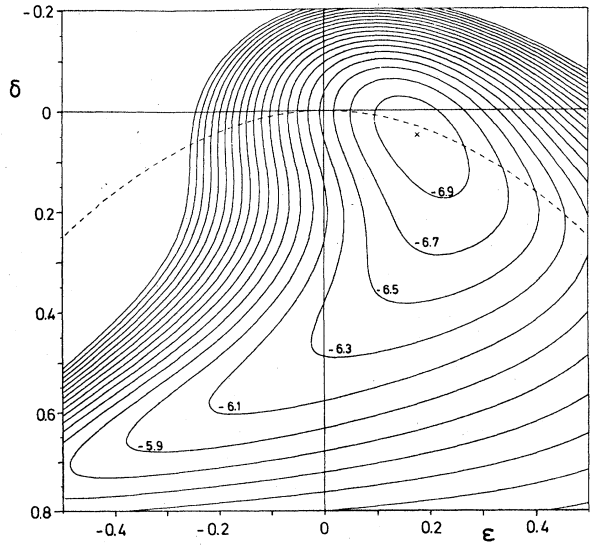

FIG. 2. Same as Fig. 1 with the physical parameters $\lambda^2=6.25$ and $V=2$.

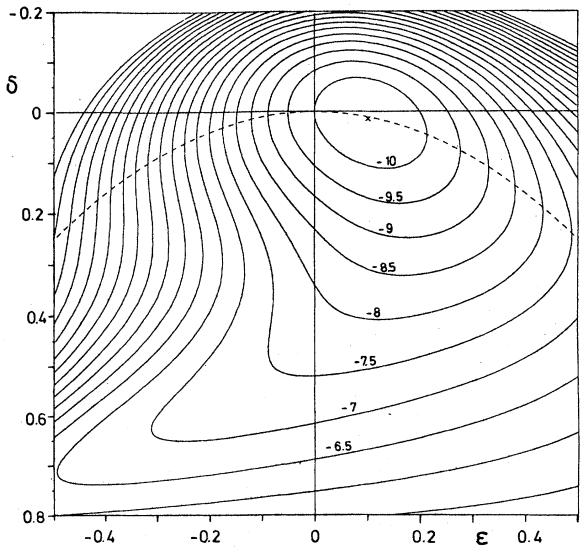

FIG. 3. Same as Fig. 1 with the physical parameters $\lambda^2=10$ and $V=2$.

(Fig. 3). Only a part of the total range of allowed values $|\epsilon| \leq 1$, $|\delta| \leq 1$ is shown. The minima in these plots correspond to the optimal choice of parameters and are marked by a cross. These figures have only one minimum. Situations where two minima exist will be discussed later.

Since our theory reduces to the simple dressed exciton theory [*ansätze* (2) and (3)] for $\epsilon=0$ the energy function corresponding to this limit emerges from the contour plots if one restricts the parameters to the vertical $\epsilon=0$ axis. Figure 2 is particularly interesting because along this axis two minima exist at $\delta\approx 0$ and $\delta\approx 0.44$. They correspond to self-trapped and mobile states. For the case shown the energies at the minima are approximately equal. If the physical parameters (λ^2 or V) are slightly varied the state of minimal energy changes discontinuously from one minimum to the other. Obviously the discontinuity vanishes if the extended theory as contained in the full contour plot is considered.

We finally remark that the dashed line in the contour plots marks the parabola $\delta=\epsilon^2$. It represents the relation $\lambda_n=-\lambda|\varphi_n|^2$ which holds for the solitary solution based on (8). Figure 3 shows that the optimized parameters almost fulfill this relation. This means that in the strong coupling or self-trapping regime the solitary solution already yields a good approximation to the ground-state energy.

V. RESULTS

In the preceding section contour plots of the energy as a function of the variational parameters ϵ and δ served to illustrate that the present theory is a considerable improvement over the simple dressed exciton theory.

In the first part of this section we present additional results on this crossover as a function of the exciton-phonon coupling strength λ^2 for the ground state ($k=0$) and an intermolecular transfer $V=2$. Figure 4 shows the ground-state energy $E(k=0)+\lambda^2$ for the three trial functions introduced in Sec. II. The simple dressed exciton theory (dashed-dotted curve) predicts two almost linear parts which are connected at a critical coupling $\lambda_c^2\approx 6.25$. The critical value depends on V, of course. The discontinuity of the first derivative of the energy with respect to λ^2 indicates the transition from the mobile to the self-trapped state within this approximation. In the strong-coupling limit ($\lambda^2 \gg \lambda_c^2$) the solitary solution (dashed line) yields an energy which is lower than the former by approximately $(V/\lambda)^2$. For weak coupling, however, it represents a worse approximation to the ground state because the energy depends quadratically on λ^2, i.e., $E_{\rm sol}\propto -\lambda^4$. For the related model Hamiltonian which describes coupling of a Frenkel exciton to acoustical phonons, the corresponding comparison of the two methods leads qualitatively to the same conclusions.[15] The present theory (solid curve) improves on both methods simultaneously and for arbitrary coupling strengths λ^2. Note that the approximate ground-state energy obtained by our approach is qualitatively very similar to the exact numerical results reported for a cyclic trimer.[21] A quantitative comparison is not possible because the initial slope depends on the number of monomers in the cyclic aggregate.

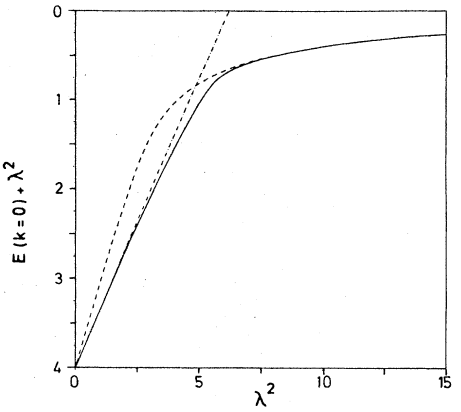

FIG. 4. Ground-state energy $E(k=0)+\lambda^2$ as a function of the Stoke's shift λ^2 for a transfer $V=2$. The present theory (solid line) is compared with the simple dressed exciton theory (dashed-dotted line) and the solitary solution (dashed line).

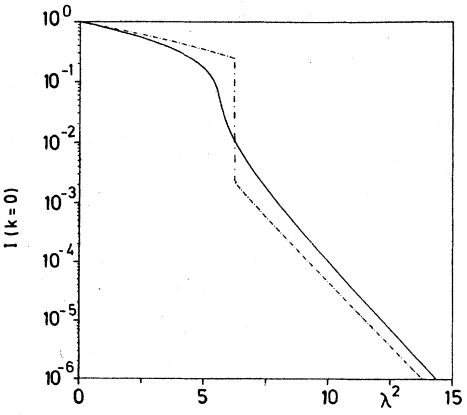

FIG. 5. Intensity of the phononless transition within the present theory (solid line) and for the simple dressed exciton theory (dashed-dotted line). $V=2$ and $k=0$ as in Fig. 4.

The continuity of the crossover between mobile and self-trapped excitons is exhibited more sensitively by the intensity of the transition from the exciton-free ground state of the crystal to the one-exciton ground state. Within our theory one has

$$I(k)=\left|\sum_n e^{-ikn}\varphi_n(k)\right|^2 \exp\left[-\sum_n \lambda_n^2(k)\right] . \tag{39}$$

Figure 5 shows $I(k=0)$ in comparison with the corresponding result for the simple dressed exciton theory (dashed-dotted line) and the same variation of the physical parameters as in Fig. 4. Again, the similarity with the exact results for short cyclic chains is striking.[21] To elucidate the situation further we include a graph of the optimized variational parameters δ [Fig. 6(a)] and ϵ [Fig. 6(b)] as a function of λ^2. The discontinuous change of the vibrational wave function as expressed by the jump of the parameter δ [dashed-dotted line in Fig. 6(a)] is replaced by a continuous variation of δ [solid line in Fig. 6(a)] and ϵ [solid line in Fig. 6(b)] in the crossover region.

A possible limitation of our theory shows up if one considers larger intermolecular couplings V, e.g., $V=5$, and looks at the behavior of the transition probability $I(k)$ as a function of λ^2. It turns out that the crossover between extended and self-trapped states now exhibits a jump discontinuity. We believe that this is due to the particular *ansatz* equations (17) and (18). It is not a result of the simplified geometric series as shown in Eqs. (32) and (33). If more parameters φ_n are varied freely the discontinuities which arise from crossing of states with the bare one-phonon states are removed. However, the discontinuity in the intensity for the $k=0$ state which shows up in Fig. (12) at $V=5$ remains.[22] It may be removed if the variational basis set is extended by inclusion of vibrationally excited states.

The second class of our results is concerned with the

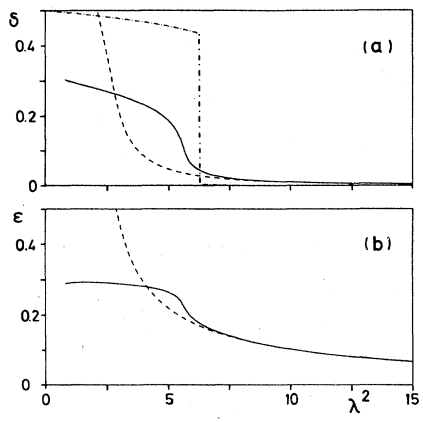

FIG. 6. Optimized variational parameters ϵ and δ as a function of λ^2 for $V=2$ and $k=0$. The curves correspond to the theories explained in the text (labeling as in Figs. 4 and 5). In the limit of vanishing coupling ($\lambda^2\to 0$) the solid curves approach (a) $\delta=0.5$ and (b) $\epsilon=0$. A jump discontinuity at $\lambda^2\approx 0.7$ is not shown in the drawings since it has no effect on the observable quantities like the energy and the intensity, cf. Figs. 4 and 5.

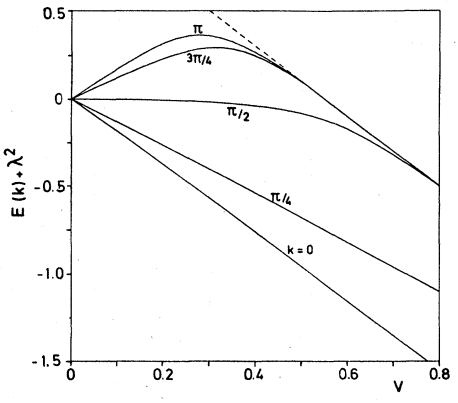

FIG. 7. Energies of the phononless exciton states as a function of the transfer V and for weak coupling $\lambda^2=0.1$. The solid curves represent different wave numbers k within the exciton band. The dashed line represents the energy of a bare exciton with $k=0$ plus a dispersionless phonon of arbitrary wave number k.

energetic and spectroscopic properties of the whole exciton band ($-\pi<k\leq\pi$) in the presence of exciton-phonon coupling.[22] Physically one expects particularly interesting effects if the lowest one-phonon state submerges into the band of bare excitons. This occurs for $V>\frac{1}{4}$ in our units. (Remember that the phonon frequency is unity.) Therefore it turns out to be most informative to study the energy $E(k)$ and the transition probability $I(k)$ as a function of the intermolecular transfer V, but at a fixed magnitude of the exciton-phonon coupling strength λ^2. We have choosen $\lambda^2=0.1$ (Figs. 7 and 8), $\lambda^2=1$ (Figs. 9 and 10), and $\lambda^2=10$ (Figs. 11 and 12) representing weak, intermediate, and strong couplings, respectively.

Let us consider the case of weak coupling ($\lambda^2=0.1$). Figure 7 shows the energy $E(k)+\lambda^2$ for various crystal wave numbers k as indicated (solid lines). For small intermolecular couplings V the dispersion relation is roughly $E(k)\approx -2V\cos k$ up to corrections proportional to λ^2. This corresponds to the bare or weakly dressed exciton. However, k is the total wave number of the system which is the sum of the excitonic and vibrational crystal momenta. Therefore, for a given k there is an almost trivial state with the same translation symmetry which consists of an exciton with wave number $k_{\rm ex}=0$ plus a phonon with wave number $k_{\rm ph}=k$ and has an energy expectation value $-2V+1$ (dashed line in Fig. 7). Since both states have the same symmetry they do not cross in the energy diagram but repell each other. Because our method is variational we only obtain the lower state which correlates to the weakly dressed exciton for small V and to the one-phonon state for larger V. This discussion qualitatively explains Fig. 7 and the evident compression of the bare exciton band $E(k)=-2V\cos k$ at the upper band edge. The information on the corresponding transition probabilities is contained in Fig. 8. The increasing one-phonon character of the states of higher k leads to an exponential decrease of the intensities. At particular values of the intermolecular transfer V the curves cease and the transition probabilities formally jump to zero. This is an artifact of our variational trial function which produces a discon-

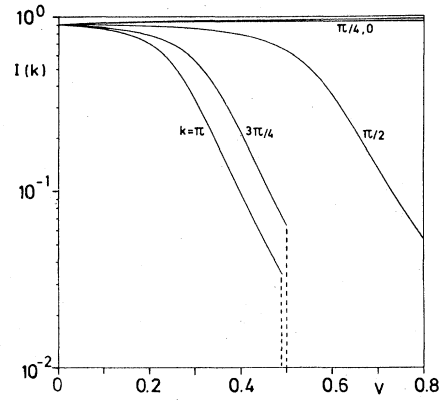

FIG. 8. Transition probabilities corresponding to the states in Fig. 7. The intensity of a given state formally jumps to zero whenever its energy joins the dashed line in Fig. 7.

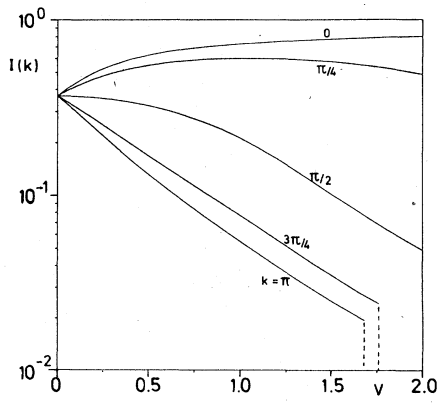

FIG. 10. Transition probabilities corresponding to Fig. 9.

tinuity of the optimized variational parameters whenever the energies become equal to the trivial one-phonon state.

Figures 9 and 10 present qualitatively similar results for an intermediate-coupling strength $\lambda^2=1$. Note that the repulsion due to the interaction with the one- and multiphonon states is much stronger than in the preceding example. The upper band edge $k=\pi$ joins the one-phonon state at larger V and even the energy of the ground state $k=0$ looses its linear dependence on V and bends down for small V. Figure 10 shows the transition probabilities. Two opposing effects of the transfer term V are observable. On the one hand, it leads to delocalization and therefore to an increasing overlap of the one-exciton ground state with the total ground state ($k=0$ and $k=\pi/4$ for small V). On the other hand, the transition probabilities tend to decrease due to the interaction with the one-phonon state ($k\geq\pi/2$ and $k=\pi/4$ but large V).

We finally consider an example of strong coupling $\lambda^2=10$ in Figs. 11 and 12. We recover the crossover between self-trapped states for small V and mobile states for $V>V_c\approx 5$. The bandwidth is extremely small (of the order $e^{-\lambda^2}$) in the first regime and the band is not resolved within the accuracy of the drawing (Fig. 11). The energy is approximately given by $E(k)\approx-\lambda^2-V^2/\lambda^2$. The term proportional to V^2 corresponds to the adiabatic approximation as contained in the soliton *ansatz* and is missing in the simple dressed exciton theory. Above critical values $V_c(k)$ which increase with k, the lower states of the band split off while strong compression of the upper part of the band remains. Figure 12 shows the transition probabilities. The ground state exhibits the jump discontinuity which is again found for strong coupling as discussed earlier in this section. Note, however, that the "hysteresis loop" corresponding to the coexisting minima turns out to be much narrower than in the simple dressed exciton theory. The crossover remains continuous for $k=\pi/4$ and larger k. It is particularly interesting that the intensity of the upper band edge is comparitively insensitive to the intermolecular transfer V. This implies a strong variation of the intensity within the band (nearly 3 orders of magnitude) for $V>V_c$. Physically the exciton at the upper band edge remains essentially self-trapped with an effective mass much larger than at the band bottom.

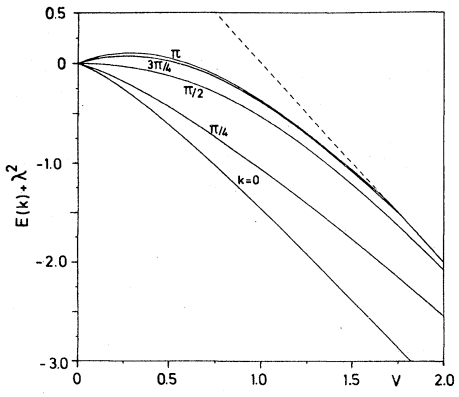

FIG. 9. Same as Fig. 7 but for an intermediate-coupling strength $\lambda^2=1$.

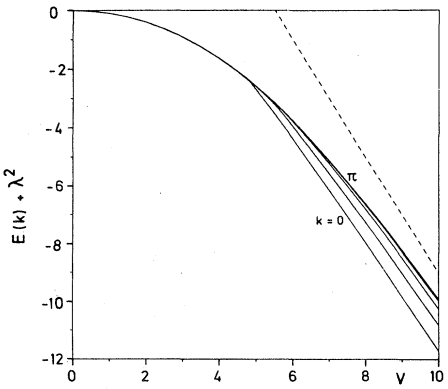

FIG. 11. Same as Fig. 7 but for strong coupling $\lambda^2=10$. The solid curves represent wave numbers $k=0$, $\pi/4$, $\pi/2$, $3\pi/4$, and π. Only the lower and the upper band edge are labeled.

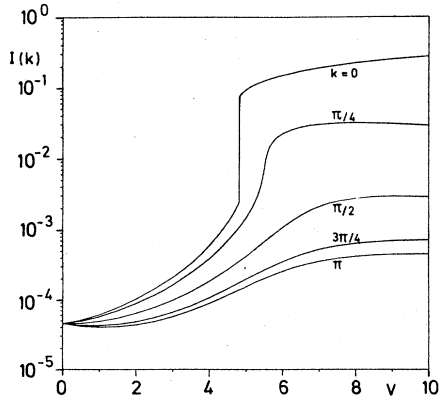

FIG. 12. Transition probabilities corresponding to Fig. 11.

VI. CONCLUSIONS

In this paper we have analyzed the excitonic states of a vibrating crystal modeled with dispersionless phonons and a linear exciton-phonon coupling. We used a variational principle with trial functions based on solitary (symmetry-breaking) states which were coherently superimposed to yield momentum-conserving (symmetry) states. The variation was performed for the superimposed states and not for the solitary *ansatz* such that electronic delocalization and lattice relaxation could be optimized independently. This approach contains the simpler dressed exciton theory and the soliton model as special limits. It is applicable to almost arbitrary electronic intermolecular and vibronic coupling energies denoted by V and λ^2, respectively. (Energies were measured in units of the phonon frequency.)

Starting from weak coupling $\lambda^2 < 1$ and $4V < 1$, it could be seen how an anticrossing behavior between the exciton states and the one- and multiphonon excitations lead to a distortion of the exciton band as a function of V on the one hand and to a small-polaron-type band for strong coupling $\lambda^2 \gg 1$ on the other hand. There are, however, considerable deviations from the small polaron picture if the electronic transfer V is also strong, $V \gg 1$. In this case the lower band edge shows indication of delocalization, that is relatively strong Franck-Condon factors, while the upper band edge represents essentially localized states of the polaron type. This difference does not only affect the dispersion within the exciton band, it also leads to different predictions about the bandwidth. The bandwidth would be $4Ve^{-\lambda^2}$ for the small polaron limit, but can be larger by several orders of magnitude in our model. Also, Holstein[19] mentioned an increase of the bandwidth beyond $4V\exp(-\lambda^2)$ for $V \gg 1$. This observation may help to understand the observed absorption spectra and effective bandwidths in PMDA crystals.[23] In addition, the strong variation of the Franck-Condon factors within the exciton band should affect the rates of radiationless interband transitions and especially their temperature dependence. Other applications concern transport properties which depend upon the degree of delocalization of the lower band eigenstates.

Of interest to us was also the crossover between self-trapped and delocalized exciton states as a function of the coupling parameters. As a measure of the degree of delocalization, we took the Franck-Condon factor to the lower band edge. We found that the discontinuity as predicted by the simplified dressed exciton model in one dimension is removed. However, a similar discontinuity reappears for much larger values of V and λ^2. To remove also these discontinuities the basic trial functions have to be extended. Earlier arguments related to the question of the transition in one dimension were based on the analysis of the adiabatic ground state within the continuum approximation.[7,9,11] Our theory goes beyond the continuum approximation and includes nonadiabatic effects.

The main application of our theory might lie in its predictive power for exciton spectra of strongly anisotropic (effectively one-dimensional) crystals, in particular, singlet transitions in systems like pseudoisocyanine[14] or inorganic complexes such as tetracyanoplatinates.[24] The intensity distribution among different states and their location can be measured quite accurately. Of course, we need to extend the model to include also vibrationally excited states. We finally point out that our method can also be applied to the coupling of excitons to acoustical phonons. This will be important for an application to transport properties and the temperature dependence of spectra at low temperatures.

*Present address: Corporate Laboratories for Information Technology, Siemens AG, D-8000 Munich, West Germany.

[1]D. P. Craig and S. H. Walmsley, *Excitons in Molecular Crystals* (Benjamin, New York, 1968).
[2]A. S. Davydov, *Theory of Molecular Excitons* (Plenum, New York, 1971).
[3]*Spectroscopy and Excitation Dynamics of Condensed Molecular Systems,* edited by V. M. Agranovich and R. M. Hochstrasser (North-Holland, Amsterdam, 1983).
[4]T. D. Lee, F. E. Low, and D. Pines, Phys. Rev. **90**, 297 (1952).
[5]Y. Toyozawa, Prog. Theor. Phys. **26**, 29 (1961).
[6]R. E. Merrifield, J. Chem. Phys. **40**, 445 (1964).
[7]D. Emin, Adv. Phys. **22**, 57 (1973).
[8]H. B. Shore and L. M. Sander, Phys. Rev. B **7**, 4537 (1973).
[9]D. Emin and T. Holstein, Phys. Rev. Lett. **36**, 323 (1976).
[10]D. Yarkony and R. Silbey, J. Chem. Phys. **65**, 1042 (1976).
[11]Y. Toyozawa and Y. Shinozuka, J. Phys. Soc. Jpn. **48**, 472 (1980).
[12]Y. Toyozawa, in *Organic Molecular Aggregates,* edited by P. Reinecker, H. Haken, and H. C. Wolf (Springer, Berlin, 1983).
[13]S. F. Fischer, in *Organic Molecular Aggregates,* edited by P. Reinecker, H. Haken, and H. C. Wolf (Springer, Berlin, 1983).
[14]P. O. J. Scherer and S. F. Fischer, Chem. Phys. **86**, 269 (1984).
[15]G. Venzl and S. F. Fischer, J. Chem. Phys. **81**, 6090 (1984).
[16]A. S. Davydov and N. I. Kislukha, Phys. Status Solidi B **75**, 735 (1976).

[17]A. S. Davydov, Physica **3D**, 1 (1981).
[18]M. A. Collins and D. P. Craig, Chem. Phys. **75**, 191 (1983).
[19]T. Holstein, Ann. Phys. (N.Y.) **8**, 325 (1959).
[20]G. Venzl (unpublished results). One proceeds as in Ref. 13.
[21]P. O. J. Scherer, W. W. Knapp, and S. F. Fischer, Chem. Phys. Lett. **106**, 191 (1984).
[22]P. O. J. Scherer and S. F. Fischer (unpublished results).
[23]D. Haarer and M. R. Philpott, in Ref. 3, p. 27.
[24]U. Rössler and H. Yersin, Phys. Rev. B **26**, 3187 (1982).